

Probing nucleon-nucleon correlations via heavy ion transfer reactions

S. Szilner^{1,a}

¹*Ruder Bošković Institute, Zagreb, Croatia*

Abstract. The revival of transfer reaction studies benefited from the construction of the new generation large solid angle spectrometers, coupled to large γ arrays. The recent results of γ -particle coincident measurements demonstrate a strong interplay between single-particle and collective degrees of freedom that is pertinent to the reaction dynamics. Via transfer of pairs, valuable information on the component responsible for particle correlations has been derived.

1 Introduction

Transfer reactions have an important impact in the understanding of correlations in the nuclear medium, and play a very important role for the study of the evolution from the quasi-elastic to the deep-inelastic and fusion regime [1]. In heavy-ion induced transfer reactions, the constituents of the collision may exchange many nucleons, thus providing information on the contribution of single particle and correlated particle transfers, and on the contribution of surface vibrations (bosons) and their coupling with single particles (fermions). Via multinucleon transfer reactions, the component responsible for particle correlations such as the pairing interaction can be studied. Although, the analysis and interpretation of these reactions can be quite complex because information about correlations is often hidden in the inclusive character of the extracted cross sections. Making use of the semi-classical approximation it has been possible to extend the concept of elementary modes of excitation in the reaction model that allowed to quantitatively study reactions that involve the transfer of many nucleons, and to predict how the total reaction cross section is shared between different channels.

The recent revival of transfer reaction studies greatly benefited from the construction of the new generation large solid angle spectrometers based on trajectory reconstruction that reached an unprecedented efficiency and selectivity. The coupling of these spectrometers with large γ arrays allowed the identification of individual excited states and their population pattern.

In this paper, some of the main advances in the field recently achieved are outlined. After a brief presentation of the experimental techniques, the main characteristics of multinucleon transfer reaction will be discussed. In particular how single particle and more complex degrees of freedom act in the transfer process.

^ae-mail: szilner@irb.hr

2 Generals on heavy ion magnetic spectrometers

Different techniques have been employed to identify nuclei produced in transfer reactions, most of them making use of magnetic spectrographs or spectrometers for a complete identification of nuclear charge, mass and energy of final reaction products. While dealing with heavier ions and weaker transfer channels, the solid angle of spectrometers increased. For such large solid angle spectrometers, in order to preserve nuclear charge and mass separation position information becomes crucial. The presently adopted solution in such cases is a simplified magnetic element configuration and the use of the concept of trajectory reconstruction. This idea has been successfully employed in the very large solid angle (~ 100 msr) spectrometers PRISMA [2–4], and VAMOS [5] and MAGNEX [6].

As an example, I here briefly recall the PRISMA spectrometer and its detection system. The reconstruction of the ion trajectory is obtained from the measurement of an entrance [2] and focal plane positions [3], together with time of flight. In between these two detector systems only two magnetic elements are located, a quadrupole followed by a dipole. The large longitudinal dimension of the dipole compared with the transversal one ensures a weak effect of the fringing fields and the planarity of the trajectory. The tracking procedure provides the curvature of ion path inside the dispersive element for a unique determination of the trajectory [4, 7]. At the end of the focal plane is located a multiparametric ionization chamber, providing nuclear charge (via ΔE) and total energy. In this way, mass and nuclear charge identification has been successfully demonstrated for ions up to $A \sim 100$ -130 (see Fig. 1), although energy resolution is presently limited to few hundreds of keV. To reach excited state discrimination for heavy ions the large solid angle magnetic spectrometers have been coupled with large γ arrays (CLARA [8], AGATA [9], EXOGAM [10]).

A very important use of such γ -particle coincidence technique is for studies of nuclei moderately far from stability whose structure is poorly known (see for example [11, 12] and refs. therein). At variance with reactions (like fusion evaporation) where the γ cascade proceeds from high-level density regions and ends-up in yrast states, grazing reactions favor a certain degree of direct population of final states, and facilitates the study of states associated with specific excitation energy or with specific structural properties.

3 Reaction mechanism

Grazing collisions produce a wealth of nuclei in a wide energy and angular range and with cross sections spanning several orders of magnitude. The determination of the absolute cross sections was crucial in order to understand how the total cross sections is divided between many open channels, and which degrees of freedom govern these processes. The quality of data and theoretical calculations presently achieved is demonstrated in Fig. 2 where it is shown, as a representative example, pick-up channels and the channels involving the one proton stripping in the reaction $^{40}\text{Ca}+^{96}\text{Zr}$ [4].

The total cross sections in Fig. 2 are compared with calculations performed with the semi-classical code GRAZING [13]. This model calculates how the total reaction cross section is distributed amongst the different reaction channels by treating quasi-elastic and deep-inelastic processes on the same footing. The GRAZING model takes into account, besides the relative motion variables, the intrinsic degrees of freedom of projectile and target. These are the surface degrees of freedom and particle transfer. The exchange of many nucleons proceeds via a multi-step mechanism of single nucleons.

Total angle and Q -value integrated cross sections for multi-neutron and multi-proton channels have been investigated with spectrometers in various systems close to the Coulomb barrier ($^{58}\text{Ni}+^{208}\text{Pb}$ [14], $^{40}\text{Ca}+^{208}\text{Pb}$ [15], $^{40}\text{Ca}+^{96}\text{Zr}$, $^{90}\text{Zr}+^{208}\text{Pb}$ [4, 16], and $^{40}\text{Ar}+^{208}\text{Pb}$ [17]). In these systems one finds that most nuclei produced in transfer reactions have N/Z ratio smaller than one of

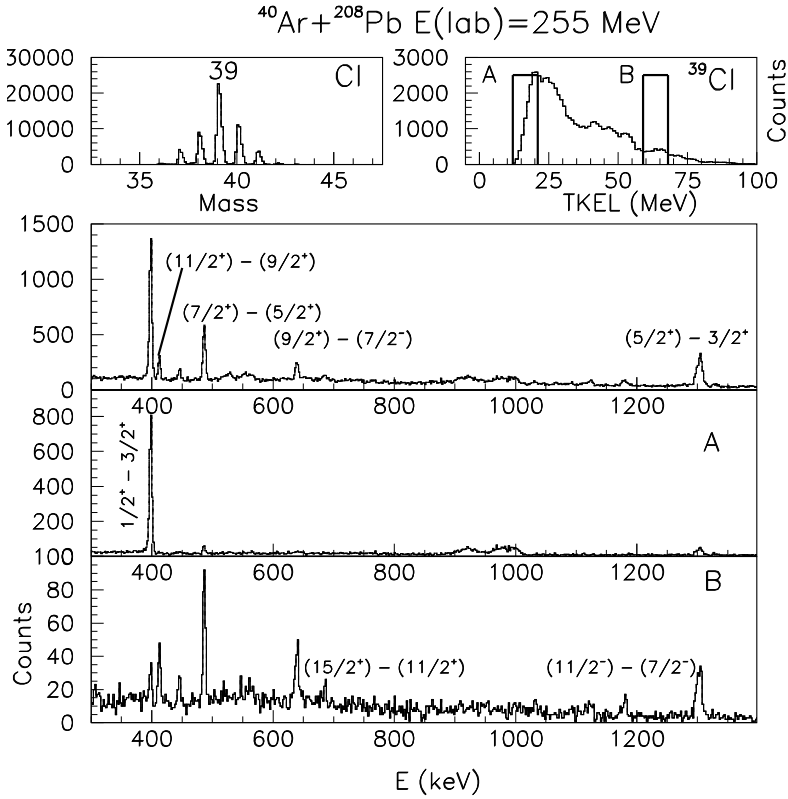


Figure 1. (Top left) Mass distribution of chlorine isotopes populated in $^{40}\text{Ar} + ^{208}\text{Pb}$ at $E_{\text{lab}} = 255$ MeV and at $\theta_{\text{lab}} = 54^\circ$ in coincidence with γ rays. A mass resolution of $\Delta A/A \sim 1/160$ has been obtained. (Top right) TKEL distribution for ^{39}Cl ($-1p$ channel) produced in the $^{40}\text{Ar} + ^{208}\text{Pb}$ reaction. (Bottom) Associated γ -ray spectra for ^{39}Cl without conditions on TKEL (top) and conditioned (middle and bottom) with different regions of TKEL distributions, marked as (A) and (B) in the TKEL spectrum.

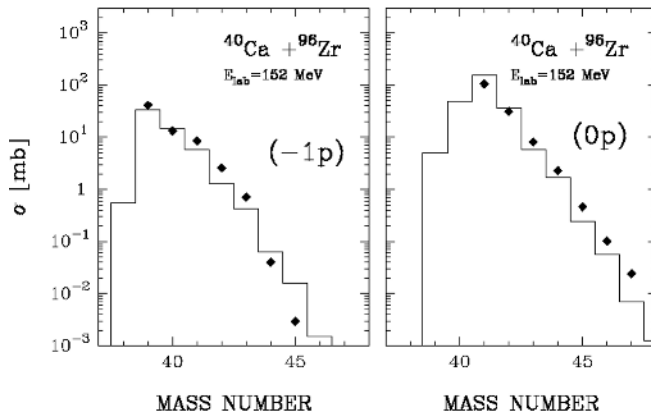


Figure 2. Total cross sections for pure neutron pick-up (right panel) and one-proton stripping (left panel) channels in the $^{40}\text{Ca} + ^{96}\text{Zr}$ reaction. The points are the experimental data and the histograms are the GRAZING code calculations (see text).

the compound nucleus, implying the dominance of a direct mechanism in the population of different fragments. For the massive proton transfer channels the isotopic distributions drift toward lower masses, a clear indication that these distributions are affected by evaporation processes. The cross sections for the neutron pick-up drop by almost a constant factor for each transferred neutron, as an independent particle mechanism would suggest. The comparison with calculations supports this idea. One can also mention that the pure proton cross sections behave differently, with the population of the $-(2p)$ channel as strong as the $-(1p)$ channel, suggesting the contribution of processes involving the transfer of proton pairs in addition to the successive transfer of single protons. This apparent proton and neutron asymmetric behavior is due to the fact that the one-neutron transfer cross section is almost one order of magnitude larger than the one-proton transfer (see Fig. 2). Thus, the contribution of a pair-transfer mode is masked, in the neutron sector, by the successive mechanism. As the very short-range pairing interaction redistributes the strength around the pure configurations, it is very important to study the yields distribution of the individual states. This subject will be addressed in next section.

4 Nucleon-nucleon correlations

Heavy-ion transfer reactions are an ideal tool for the study of the residual interaction in nuclei, in particular the components responsible for the couplings between the single particle and phonon degrees of freedom, as well as particle correlations. Below, the recent studies on the subjects will be discussed.

4.1 Particle vibration couplings

The coupling of single-particle degrees of freedom to nuclear vibration quanta is essential for the description of many basic states in the vicinity of closed shells. The effects of such coupling are largely unexplored, in particular, whether and to what extent a population of states of particle-phonon nature is present in isotopic chains reached via multiple-particle transfer mechanism. The Ar (neutron transfer channels) [18] and Cl [19] (one proton stripping channels) isotopes have been populated in the $^{40}\text{Ar}+^{208}\text{Pb}$ reaction. Their γ spectra display strong transitions which can be connected with the single-particle or single-hole states. In addition, through the whole isotopic chain also states that involve combinations of a single particle or hole with a collective boson have been populated. For example, in ^{40}Ar one notices a very strong population of the 2_1^+ state. In ^{41}Ar , the one-neutron transfer channel, beside the low lying states with a pronounced single-particle character, as the $3/2_1^-$ state, the decay of the $11/2^-$ state has been observed. Similarly occurs in other populated odd Ar isotopes (see Fig. 3 top panel).

These $11/2^-$ states can be understood as a coupling of a collective boson to single-particle states (i.e. $|2^+, (f_{7/2})^1 \rangle$) giving a $11/2^-$ stretched configuration. The properties of such states are closely connected with the properties of the vibration quanta, allowing one to follow the development of collectivity in odd isotopic chain, a phenomenon widely discussed in even-even isotopes (see Fig. 3 top panel). The significant population of states that match a stretched configuration of the valence neutron coupled to the vibration quanta, demonstrates the importance of the excitation of the states whose structure can be explained with the same degrees of freedom which are needed in the reaction model: surface vibrations, and single particles. It is through the excitation of these modes that energy and angular momentum are transferred from the relative motion to these intrinsic degrees of freedom and that mass and charge are exchanged among the two partners of the collision.

In recent years, a special interest was dedicated to the breakdown of the $N = 28$ magic number, or vanishing of the proton $Z = 16$ sub-shell gap [21, 22]. The behavior of the proton $s_{1/2}$ and $d_{3/2}$

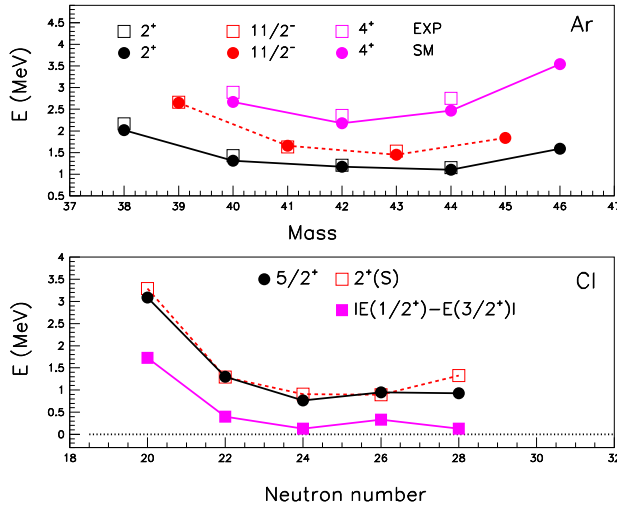


Figure 3. (Top): Energies of the 2^+ , 4^+ and $11/2^-$ states of argon isotopes with $N = 20-28$. Solid circles are SM calculated energies, open squares are the adopted levels, whereas open triangles correspond to the energies of $11/2^-$ in ^{41}Ar and ^{43}Ar from Refs. [18, 20]. In the most recent compilation of the ^{45}Ar level properties, a level at 1911(5) keV is a good candidate for the $11/2^-$ state, and was added (cross symbol) for completeness. (Bottom): Absolute energy difference between the lowest $1/2^+$ and $3/2^+$ states in the odd-even chlorine isotopes (filled squares, violet) and excitation energies of the $5/2^+$ states (filled circles, black), compared with the energies of the 2^+ states in S isotopes (empty squares, red), as a function of the neutron number. Curves are here only to guide eyes.

orbitals was crucial in understanding these effects. In chlorine nuclei one expects that the $s_{1/2}$ orbital is completely filled and that the unpaired proton occupies the $d_{3/2}$ orbital. Figure 1 shows the γ spectra of the ^{39}Cl isotope, where the strongest line belongs to the decay of the $1/2^+$ state to the ground $3/2^+$ state, with a dominant single particle configurations. With increasing neutron number, the $d_{3/2} - s_{1/2}$ splitting is reduced and mixing between different proton configurations increases. This mixing results in nearly quasi-particle states, and the heavy Cl isotopes can be viewed as one proton coupled to the corresponding $(A-1)\text{S}$ isotope, or to the quadrupole excitation. This behavior in Cl isotopes can be demonstrated by inspecting the $5/2^+$ states (see Fig. 3 bottom panel) [19]. A similar trend of the energies of the higher spin states, $7/2^+$ and $9/2^+$, has been observed.

A strong excitation of the states whose dominant structure can be viewed as a particle or hole coupled to the quadrupole or octupole excitation has been also observed in many other isotopic chain populated by the multi-nucleon transfer reactions [11, 23–25].

4.2 Sub-barrier transfer reactions

With heavy ions, as previously stressed, multiple transfer of nucleons becomes available in the reaction, giving the possibility to study the relative role of single particle and pair transfer modes. Of particular interest is still whether it is possible to reach a situation where multiple transfer of pairs

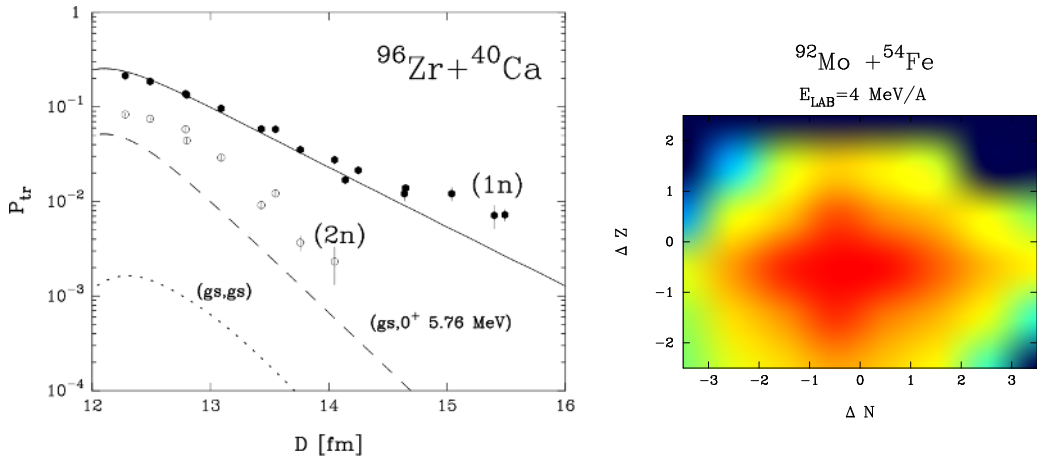


Figure 4. (Left): Theoretical transfer probabilities for one- and two-particle transfer (lines) in comparison with the experimental data (points) measured in $^{96}\text{Zr} + ^{40}\text{Ca}$. The full line represents the inclusive transfer probability for one-neutron transfer, the dotted line the ground-ground state transition for the two-neutron transfer, and the dashed line the transition to the 0^+ excited state at ~ 6 MeV in ^{42}Ca . (Right): Total cross section in the ΔN (number of transferred neutrons) vs. ΔZ (number of transferred protons) matrix calculated with the code GRAZING for the $^{92}\text{Mo} + ^{54}\text{Fe}$ reaction. Positive and negative numbers correspond to pick-up and stripping channels, respectively.

are dominating the exchange of mass and charge between the interacting nuclei (Josephson effect). The problematics connected with the pair correlations is of current interest in ongoing research with radioactive beams, where the pairing interaction is expected to be significantly modified in nuclei with extended neutron distributions [26–28].

At energies below the Coulomb barrier, even though the cross sections are much smaller than the ones encountered at higher energies, certain advantages appear when dealing with energies for which the interacting nuclei cannot overcome their mutual Coulomb barrier. The interacting nuclei are only slightly influenced by the nuclear potential and Q values are restricted to few MeV for the open transfer channels. These conditions diminish the complexity of coupled channel calculations and quantitative information may be extracted on the nucleon-nucleon correlations even from inclusive measurements.

The coming into operation of large acceptance magnetic spectrometers made it possible to perform measurements on multinucleon transfer reactions with good ion identification also at very low bombarding energies. From the experimental point of view, at energies below the barrier measurements of heavy-ion transfer reactions products present significant technical difficulties. Backscattered ions have low kinetic energies which severely limit their identification, making available data extremely scarce. A new series of measurements have been successfully started by exploiting the large acceptance of the spectrometer PRISMA and by employing inverse kinematics: $^{96}\text{Zr} + ^{40}\text{Ca}$ [16], and $^{116}\text{Sn} + ^{60}\text{Ni}$ [29], and $^{92}\text{Mo} + ^{54}\text{Fe}$ [30]. With detection at very forward angles, one has, at the same time, enough kinetic energy of the outgoing recoils (for energy and therefore mass resolution) and forward focused angular distribution (high efficiency). In these measurements a significant transfer yield could be detected at the level of 10^{-4} with respect to the elastic channel.

Results of the measurement of the $^{96}\text{Zr} + ^{40}\text{Ca}$ system (closed shell nuclei) are presented, together with the microscopic calculations, in Fig. 4 (left panel) for $+(1n)$ and $+(2n)$ neutron transfer channels via transfer probabilities as a function of the distance of closest approach. To compute the inclusive

one-neutron stripping cross section (full line) the transfer probability by summing over all possible transitions in projectile and target has been calculated. One sees how calculations reproduce well the experimental slope as well as the absolute values of the transfer probabilities for the one neutron channel.

For the two particle transfer [16], the model takes into account the successive and simultaneous transfers, where only two-particle configuration coupled to 0^+ (i.e. transfer of a $J = 0^+$ pair) is included. In Fig. 4 (left panel), a dotted line shows the calculated probability for the ground-to-ground state transition. Clearly, this transition does not contribute to the total transfer strength in agreement with what was experimentally observed in the Q -value spectra [16, 31]. In the same figure, with a dash line, is shown the predicted transfer probability for the transition to the 0^+ state at ~ 6 MeV in ^{42}Ca . It is apparent that the contribution of this transition is much larger than the ground state one. At present the still remaining enhancement factor is ascribed to the fact that the two-nucleon transfer reaction does not populate only 0^+ states but it is much richer, so that more complicated two-particle correlations have to be taken into account.

At variance with the $^{96}\text{Zr}+^{40}\text{Ca}$ system (closed shell), in the $^{116}\text{Sn}+^{60}\text{Ni}$ system (super-fluid nuclei) [29], the ground to ground state Q values for neutron transfers is close to zero, matching the optimum Q -value (~ 0 MeV). The comparison between data and theory for these two cases, namely nuclei near closed shells and nuclei of super-fluid character, which will significantly improve our understanding of the origin of the enhancement factors, is in progress.

In this context, it is also important to investigate the role played by neutron-proton correlations. Nuclear models point out that such a correlation is expected to be strongest in $N \sim Z$ nuclei, where protons and neutrons occupy the same orbitals [32]. As known, multinucleon transfer reactions allow the transfer of large number of nucleons, and the strength of each of these channels is governed by form factors and optimum Q -value consideration. In order to study proton-neutron correlation one has to use systems where the population of the (np) channels is allowed by the Q -value. Thus, pair-correlation properties not only in the neutron transfer channels but for all possible nucleon correlations, $\pm(nn)$, $\pm(pp)$ and $\pm(np)$ channels, have been tested at the same time, by working below the barrier. The $^{92}\text{Mo}+^{54}\text{Fe}$ system is amongst the best choices (see Fig. 4 right panel) which cope well with the peculiar experimental constraints of the inverse kinematic measurement at sub-barrier energies, and which comes as close as heavy-ion induced transfer reactions allow to the $N = Z = 27$ region. Preliminary results display an enhancement in the $+pn$ channel, when compared with the simple expectation of the independent proton and neutron transfers. More detailed analysis and comparison with the semi-classical models are in progress.

5 Summary

The advent of the last generation large solid angle magnetic spectrometers, coupled to large γ arrays, ensured significant advances in the field of multinucleon transfer reactions at energies close to the Coulomb barrier. Via multiple transfers of neutrons and protons one can populate nuclei moderately far from stability, especially in the neutron-rich region, and thus study this yet unexplored part of the nuclear chart. From the point of view of the mechanism, present focus is also on the study of the production and properties of the heavy binary partner. Of special interest is to get access to neutron rich heavy nuclei, important also for astrophysics. Even with the presence of secondary effects, namely nucleon evaporation and transfer induced fission, which lower the final yield, multi-nucleon transfer reactions still provide a sufficient cross sections especially in the regions where other production methods, like fission or fragmentation, have severe limitations or cannot be used at all. These studies will be of increasing relevance for the ongoing and foreseen experiments with radioactive beams.

ACKNOWLEDGMENTS

The material presented in this conference is the result of a cooperative work of many people of the PRISMA+CLARA/AGATA collaboration and belonging to different institutions (LNL, Padova, Torino, Zagreb, Bucharest, Strasbourg) which I wish to acknowledge. This work was partly supported by the EC FP6 EURONS Contract No. RII3-CT-2004-506065, and FP7-REGPOT PD Contract No.256783 projects.

References

- [1] L. Corradi, G. Pollarolo, and S. Szilner, *J. of Phys. G* **36**, 113101 (2009).
- [2] G. Montagnoli *et al.*, *Nucl. Instrum. Methods A* **547**, 455 (2005).
- [3] S. Beghini *et al.*, *Nucl. Instrum. Methods A* **551**, 364 (2005).
- [4] S. Szilner *et al.*, *Phys. Rev. C* **76**, 024604 (2007).
- [5] H. Savajols *et al.*, *Nucl. Phys. A* **654**, 1027c (1999).
- [6] A. Cunsolo *et al.*, *Nucl. Instrum. Methods A* **481**, 48 (2002).
- [7] D. Montanari *et al.*, *Eur. Phys. J. A* **47**, 4 (2011).
- [8] A. Gadea *et al.*, *Eur. Phys. J. A* **20**, 193 (2004).
- [9] A. Gadea *et al.*, *Nucl. Instrum. Methods A* **654**, 88 (2011).
- [10] S. L. Shepherd *et al.*, *Nucl. Instrum. Methods A* **434** (1999) 373.
- [11] S. Lunardi *et al.*, *Phys. Rev. C* **76**, 034303 (2007).
- [12] J. J. Valiente-Dobón *et al.*, *Phys. Rev. Lett.* **102**, 242502 (2009).
- [13] A. Winther, *Nucl. Phys. A* **572**, 191 (1994); *Nucl. Phys. A* **594** 203 (1995); program GRAZING, <http://www.to.infn.it/~nanni/grazing>.
- [14] L. Corradi *et al.*, *Phys. Rev. C* **66**, 024606 (2002).
- [15] S. Szilner *et al.*, *Phys. Rev. C* **71**, 044610 (2005).
- [16] L. Corradi *et al.*, *Phys. Rev. C* **84**, 034603 (2011).
- [17] T. Mijatović *et al.*, *Nuclear Structure and Dynamics 2012*, AIP Conf. Proc. **1491**, 346 (2012).
- [18] S. Szilner *et al.*, *Phys. Rev. C* **84**, 014325 (2011).
- [19] S. Szilner *et al.*, *Phys. Rev. C* **87**, 054322 (2013).
- [20] D. Mengoni *et al.*, *Phys. Rev. C* **82**, 024308 (2010).
- [21] O. Sorlin and M.-G. Porquet, *Prog. Part. Nucl. Phys.* **61**, 602 (2008).
- [22] E. Caurier, G. Matrinez-Pinedo, F. Nowacki, A. Poves, and A. P. Zuker, *Rev. Mod. Phys.* **77**, 427 (2005).
- [23] D. Montanari *et al.*, *Phys. Lett. B* **697**, 288 (2011).
- [24] F. Recchia *et al.*, *Phys. Rev. C* **85**, 064305 (2012).
- [25] S. Bhattacharyya *et al.*, *Phys. Rev. C* **79**, 014313 (2009).
- [26] J. Dobaczewski *et al.*, *Phys. Rev. Lett.* **72**, 981 (1994).
- [27] I. Tanihata *et al.*, *Phys. Rev. Lett.* **100**, 192502 (2008).
- [28] G. Potel *et al.*, *Phys. Rev. Lett.* **105**, 172502 (2010).
- [29] D. Montanari *et al.*, *Journal of Physics: Conference Series* **420** 012127 (2013).
- [30] S. Szilner *et al.*, INFN - LNL PAC proposal.
- [31] S. Szilner *et al.*, *Eur. Phys. J. A* **21**, 87 (2004).
- [32] P. Van Isaker, D. D. Warner and A. Frank, *Phys. Rev. Lett.* **94**, 162502 (2005).